AD-778 326

EXCIMER FORMATION AND DECAY PROCESSES IN RARE GASES

Donald C. Lorentz, et al

Stanford Research Institute

Prepared for:

Office of Naval Research

28 September 1973

STANFORD RESEARCH INSTITUTE
Menlo Park, California 94025, U.S.A.

Final Report *September 28, 1973*

EXCIMER FORMATION AND DECAY PROCESSES IN RARE GASES

SRI =MP 73-2

By: D. C. LORENTS, D. J. ECKSTROM and D. HUESTIS

Prepared for:

THE OFFICE OF NAVAL RESEARCH
DEPARTMENT OF THE NAVY
800 NORTH QUINCY STREET
ARLINGTON, VIRGINIA 22217

CONTRACT N00014-72-C-0457
NRL Req. 00173-2-006435/4-19-72
EAM TITLE: VAN DER WAALS LASERS

SRI Project PYU-2018

Approved by:

FELIX T. SMITH, *Manager*
Molecular Physics

CHARLES J. COOK, *Executive Director*
Physical Sciences Division

Unclassified
Security Classification

DOCUMENT CONTROL DATA - R & D

Security classification of title, body of abstract and indexing annotation must be entered when the overall report is classified.

1 ORIGINATING ACTIVITY (Corporate author)
Stanford Research Institute
333 Ravenswood Avenue
Menlo Park, California 94025

2a. REPORT SECURITY CLASSIFICATION
Unclassified

2b. GROUP

3 REPORT TITLE

EXCIMER FORMATION AND DECAY PROCESSES IN RARE GASES

4 DESCRIPTIVE NOTES (Type of report and inclusive dates)

Final Report

5 AUTHOR(S) (First name, middle initial, last name)

Donald C. Lorents, Donald J. Eckstrom, and David L. Huestis

6 REPORT DATE	7a. TOTAL NO OF PAGES	7b. NO OF REFS
September 28, 1973	68	38

8a CONTRACT OR GRANT NO	9a. ORIGINATOR'S REPORT NUMBER(S)
N0014-72-C-0457	SRI MP73- 2
b. PROJECT NO	
c.	9b. OTHER REPORT NO(S) (Any other numbers that may be assigned this report)
d	

10 DISTRIBUTION STATEMENT

Distribution of this document is unlimited.

APPROVED FOR PUBLIC RELEASE
DISTRIBUTION UNLIMITED

11 SUPPLEMENTARY NOTES

12 SPONSORING MILITARY ACTIVITY
Office of Naval Research
Department of Navy
Arlington, Virginia 22217

13 ABSTRACT

A model of the excimer formation and decay processes in electron beam pumped high density rare gases has been developed. The model has been compared with recent measurements of the excimer formation and decay rates in Xe and information about the radiative lifetimes and dominant collision mechanisms are obtained. Several important conclusions that have bearing on the vuv laser characteristics of these systems are discussed.

14 KEY WORDS	LINK A		LINK B		LINK C	
	ROLE	WT	ROLE	WT	ROLE	WT
vuv laser						
Excimer laser						
dissociation laser						
Rare gas laser						
e-beam pumping						

TABLE OF CONTENTS

LIST OF ILLUSTRATIONS

LIST OF TABLES

SUMMARY

The purpose of this program is to develop an understanding of the molecular kinetics pertinent to new high efficiency, high power lasers. We are studying high pressure gases that are initially pumped by intense bursts of electrons (such as 10^3 amperes, 500 keV, 3×10^{-9} sec), since these systems could have efficiencies of more than 10% and also short pulse, high power capability. This energy, which is primarily deposited by creating atomic ions, rapidly collects in the lowest molecular excited state. Laser radiation from this state is possible either when the ground state is repulsive, that is, when no bound, ground molecular state exists (e.g., the rare gases and Hg, Cd, and Zn), or when the upper laser state radiates primarily to higher vibrational levels of the ground state.

The high pressure rare gases show considerable promise of providing highly efficient media for high powered laser action in the ultraviolet wavelength range. However, since the excimer radiation is a continuum with a bandwidth on the order of 100 Å, the optical gain is orders of magnitude smaller for a given population inversion than comparable discrete transitions and, correspondingly, larger upper state populations are required. Therefore, a large part of our research effort has been

directed at determining the conditions for obtaining high excimer densities with high efficiency. Various loss processes have been suggested which would limit laser efficiency. These include excimer-excimer Penning ionization, excimer photoionization, quenching by ground state atoms, and absorption by ground state molecules. A corresponding effort has been devoted to determine the importance of these loss processes and their effect on laser operation.

The major result has been the development of a theoretical model for excimer formation and decay following short pulse electron beam excitation of Ar and Xe at pressures above 1 atm. The model has been developed on the basis of existing knowledge of electron, ion, and excited atom interactions in rare gases, together with available experimental information on the behavior of high pressure rare gases excited by charged particles. The basic framework of the reaction scheme is believed to be well established although some details remain to be filled in and some of the rate constants need to be determined. The important areas where knowledge is lacking are pointed out and the reactions that are particularly important in limiting the performance as a laser medium are emphasized. The model has been used to calculate excimer formation and decay rates in Xe at different pressures and the results are compared to recent experimental data obtained under Febetron excitation conditions.

On the basis of our studies we have reached the following conclusions:

(1) The $^1\Sigma_u^+$ excimer is the upper level of the lasing transition.

(2) The photoionization cross section of the $^3\Sigma_u^+$ excimer level probably exceeds its stimulated emission cross section. This would make the $^3\Sigma_u^+$ population act as an absorber of the singlet radiation.

(3) Rapid (electron induced) mixing of the $^1\Sigma_u^+$ and $^3\Sigma_u^+$ states is implied by the observed decay behavior. This would be a necessary condition to insure a population in the $^1\Sigma_u^+$ level sufficient for lasing.

(4) Quenching of the excimers by ground state atoms does not appear to be an important loss mechanism.

(5) Excimer-excimer Penning ionization remains a significant limitation on laser efficiency.

I INTRODUCTION

The excitation of high density rare gases by energetic charged particles, resulting in radiation in the vacuum ultraviolet region, has been of interest to radiation physicists for a long time. In these high density collision-dominated systems, the electronic excitation energy is quickly and efficiently converted to excited diatomic molecules known as excimers. These excimer states radiate in a narrow vuv continuum band by making a transition to a repulsive ground state that promptly dissociates. These unique properties of the excited high density rare gases are important in a number of potential applications. One of these is the vuv dissociation laser, the feasibility of which has already been demonstrated for Kr and Xe.[1-4] A second promising application is the use of these systems as efficient incoherent uv sources, which can be used as laser pumps and for photochemistry studies. A third laser oriented application being investigated is the use of the excimer states to excite other molecules by means of energy transfer collisions.[5] This appears to be an efficient means of producing inversions on transitions in various atomic and molecular species. By this means it appears possible to design and operate efficient lasers at many different wavelengths.

To capitalize on these applications it is essential to have a clear physical and quantitative understanding of the mechanisms of energy deposition, and of excimer formation and relaxation in the pure high pressure rare gases. Equally important is an understanding of the state structure and radiative properties of the rare gas dimer. The objectives of this study have been to investigate the structure and the important mechanisms, delineate the chain of reactions, and develop a model for these processes that serves as the basis for a computer code. These objectives have been reached, and although many details remain to be ascertained and many reaction rates are unknown, it is possible to explain reasonably all the observations with one consistent model. Further, we have developed a computer code that calculates the excimer density as a function of time following a short excitation pulse. The results have been compared with the experimentally measured decay rates of Koehler et al.,[6] and good agreement is attained over an extremely wide pressure range.

II ANALYTICAL MODEL

Excimer State Structure

Guided by Mulliken's state structure diagram for Xe_2,[7] we estimated the electronic state structure of Ar_2 from available scattering data, spectroscopic data, and theoretical calculations. The resulting curves were presented in our semiannual technical report.[8] Since that time, the well depths of the Ar_2^+ and Xe_2^+ attractive potentials were measured in our laboratory.[9]

In the case of Ar_2^+ our measurements confirmed the calculations of Gilbert and Wahl[10] that had been used in the construction of the Ar_2 states reported previously, giving added confidence in those results. For Xe, we can use the measured Xe_2^+ well depth, together with the calculated ground state potential curve and the radiative transition energy (i.e., λ = 1716 Å) to place limits on the Xe_2^* excimer potential. We find that the excimer potential must lie within the limits: ϵ = 0.97 eV, R_e = 3.39 Å and ϵ = 0.75 eV, R_e = 3.12 Å, where ϵ and R_e are the well depth and equilibrium internuclear separation, respectively. The well depths for both Xe_2^* and Ar_2^* could be measured directly by scattering techniques, and this important measurement should be made in the near future!

With respect to the laser application, one of the most important characteristics of the state structure of Xe_2, Kr_2, and Ar_2 is the existence of two close-lying radiative excimer states. These states are closely spaced, and the ground state is so steep that the radiation appears as a single band that cannot be spectrally resolved into two components. It is expected that radiation from the upper singlet state is fully allowed, whereas the lower triplet state will be longer lived. The current status of experimental and theoretical work on the lifetimes is discussed fully in Section III. The effect of spin-orbit splitting on the excimer potential curves is discussed in detail in the following subsection.

Spin-Orbit Sublevels of the Rare Gas Excimers

Mulliken[7] provided a qualitative description of the Xe_2 excimer levels arising from the $5p^5 6s$ and $5p^5 6p$ atomic configurations. To improve the usefulness of his analysis, we performed a semiempirical calculation of the spin-orbit splittings in the $5p^5 6s$ molecular levels. This calculation has also been made for the excimer levels of Kr_2^*, Ar_2^*, and Ne_2^*. (A similar calculation of the spin-orbit levels in Hg_2^* was described in a previous report.[5]) The $p^5 s$ configuration gives rise to four atomic fine structure levels in each of the rare gases. In Ne^*, these are simply described in Russell-Saunders notation by $^1P_1$, $^3P_0$, $^3P_1$, and $^3P_2$. In Xe^* they would be called $(\frac{1}{2})_1$, $(\frac{1}{2})_0$, $(\frac{3}{2})_1$, $(\frac{3}{2})_2$. In forming the

excimer molecule, say Xe_2^*, each of these atomic sublevels produces a mixture of Σ and Π components when projected onto the internuclear axis. In the molecule the atomic angular momentum is no longer conserved, but rather only its internuclear projection. At large internuclear separation L or S remain coupled and the projection of J along the internuclear axis is the conserved quantity (Hund's case c or d). As the internuclear distance is reduced, the orbital angular momentum uncouples from the spin and couples instead with the internuclear axis (Hund's case a or b). The states make a gradual transition from Hund's cases (c) and (d) to cases (a) and (b).

Decomposing the ^3P_J and $^1P_1$ levels into their Σ and Π components allows us to set up the matrix Hamiltonians to be diagonalized. These are shown in Table I. We use the notation of Condon and Shortley,[11] where ζ is the spin-orbit splitting parameter, G is the singlet-triplet splitting parameter, and W is a new parameter to designate the Σ-Π splitting. The values of ζ and G can be found by fitting the atomic energy levels as reported by Moore.[12] To calculate the relative energies of the molecular spin-orbit levels using the atomic parameters, we must assume that the spin-orbit interaction does not change drastically as a result of molecular distortion. These changes are expected to be small, particularly for the low-lying excimer levels, 0_u^+, 1_u, 0_u^-.

Table I

MOLECULAR SPIN-ORBIT MATRICES FOR sp OR p^5s ATOMIC CONFIGURATIONS

O^-	$^3P_0^0$	$^3P_2^0$
$^3P_0^0$	$\frac{W}{6} - \zeta - G$	$\sqrt{\frac{2}{9}}\, W$
$^3P_2^0$	$\sqrt{\frac{2}{9}}\, W$	$-\frac{W}{6} + \frac{\zeta}{2} - G$

O^+	$^1P_1^0$	$^3P_1^0$
$^1P_1^0$	$-\frac{W}{2} + G$	$\sqrt{\frac{1}{2}}\, \zeta$
$^3P_1^0$	$\sqrt{\frac{1}{2}}\, \zeta$	$\frac{W}{2} - \frac{\zeta}{2} - G$

1	$^3P_2^1$	$^3P_1^1$	$^1P_1^1$
$^3P_2^1$	$\frac{\zeta}{2} - G$	$-\frac{W}{2}$	0
$^3P_1^1$	$-\frac{W}{2}$	$-\frac{\zeta}{2} - G$	$\sqrt{\frac{1}{2}}\, \zeta$
$^1P_1^1$	0	$\sqrt{\frac{1}{2}}\, \zeta$	$\frac{W}{2} + G$

2	$^3P_2^2$
$^3P_2^2$	$\frac{W}{2} + \frac{\zeta}{2} - G$

SA-1925-34

Figures 1 and 2 show the relative energies of the molecular spin-orbit levels of Ar_2^* and Xe_2^* arising from Ar ($3p^5 4s$) on Ar ($3p^6$) and Xe ($5p^5 6s$) on Xe ($5p^6$), respectively. The ordering and approximate energy separation of the states are shown as a function of the Σ-Π splitting energy. The Σ-Π splitting itself is expected to vary with R approximately as the overlap of one atom with the other, or about exponentially. As Mulliken suggests, we expect the Σ_u states to be lower than the Π_u states; hence, the Σ-Π splitting is taken to be positive. Correspondingly, the Σ_g states should be higher than the Π_g states, and in that case the splitting is negative.

Important conclusions from these calculations include the following:

(1) The splitting between the $^3\Sigma_u^+$ and $^1\Sigma_u^+$ excimer levels should be about the same for the various rare gases, about 1600 cm^{-1}.

(2) The splitting between the 0_u^- and 1_u sublevels of the $^3\Sigma_u^+$ state should be quite small at R_e: in Ne_2^* < 1 cm^{-1}, Ar_2^* < 3 cm^{-1}, Kr_2^* < 25 cm^{-1}, Xe_2^* < 80 cm^{-1}.

(3) Potential barriers are expected as a result of spin-orbit mixing in the 0_u^+ curves of Ne_2^* (350 cm^{-1}) and Ar_2^* (160 cm^{-1}). The actual barrier in Ar_2^* appears to be smaller (60-140 cm^{-1}, ref 13), because of long-range electrostatic attraction. These barriers may have serious consequences for the kinetics of excimer formation.

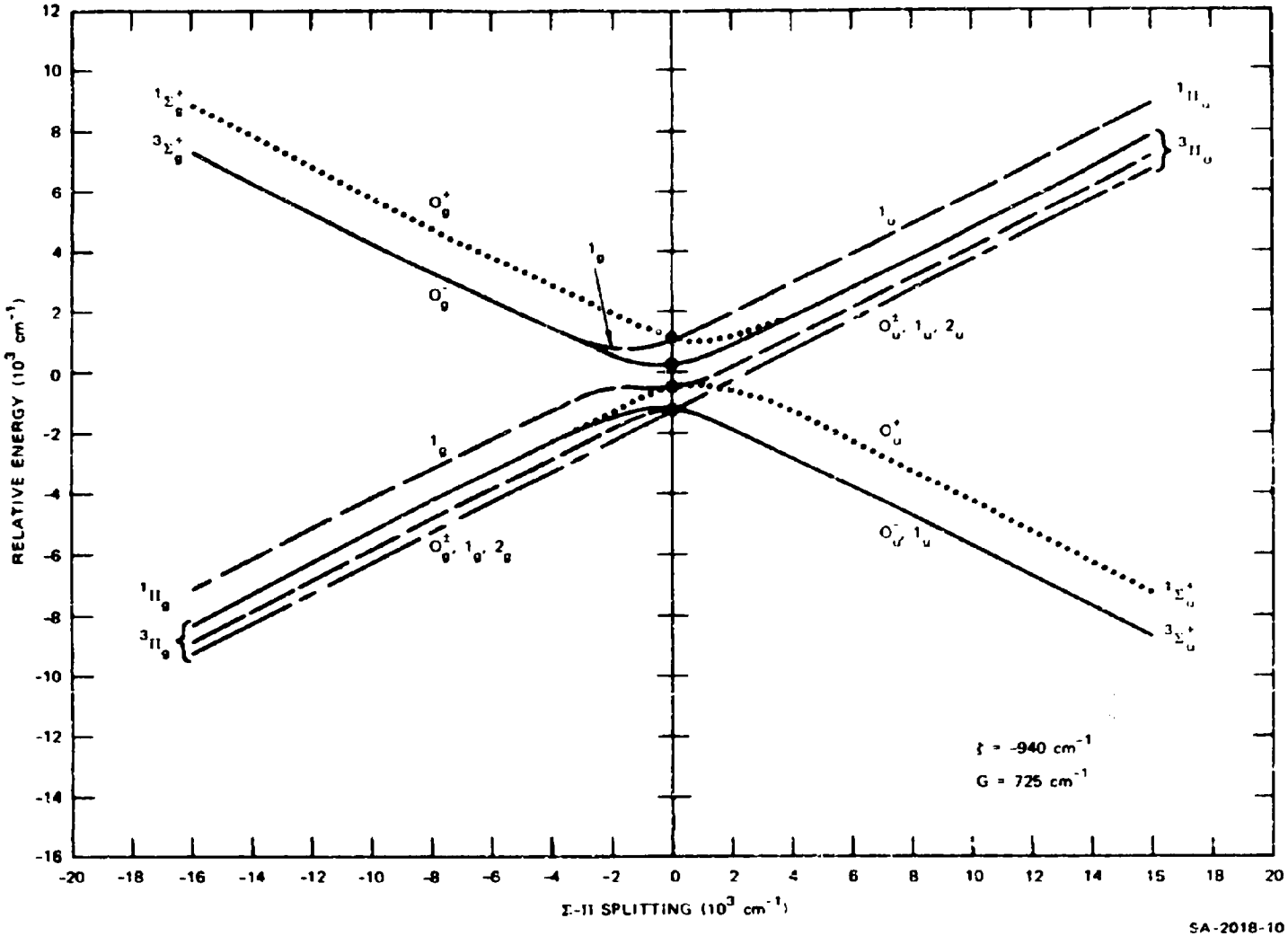

FIGURE 1 SPIN ORBIT LEVEL DIAGRAM FOR Ar_2^*

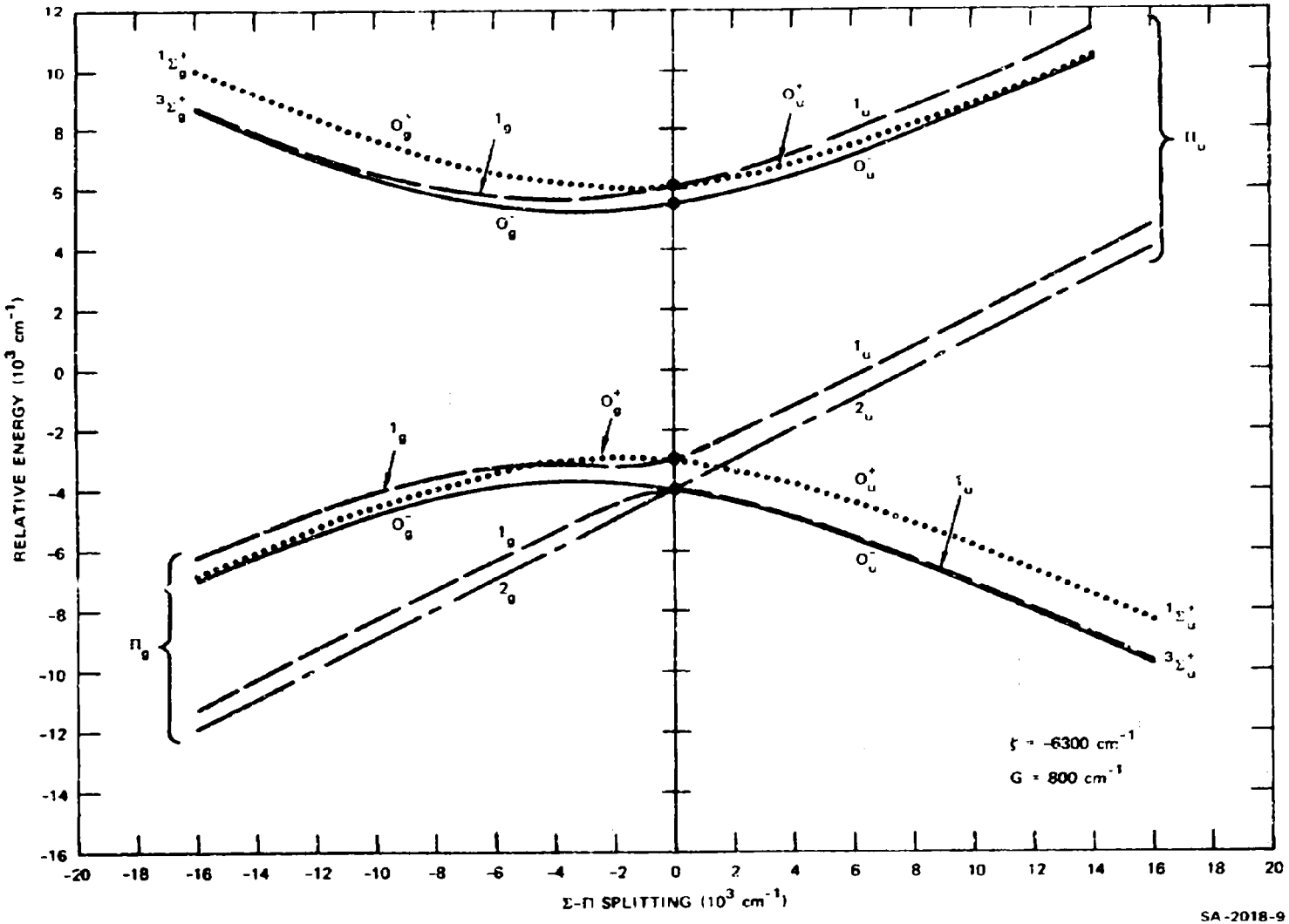

FIGURE 2 SPIN ORBIT LEVEL DIAGRAM FOR Xe_2^*

(4) No barriers are predicted for the 0_u^+ states of Kr_2^* and Xe_2^*, nor are any predicted for the 1_u and 0_u^- excimer levels for all four rare gases.

(5) Finally, we can estimate the relative transition strengths of the various 0_u^+ and 1_u levels by determining the amount of $^1\Sigma_u^+$ and $^1\Pi_u$ character in the wave function for each state. The results of this calculation are discussed in Section III.

Reaction Model and Rates

The model of the flow of energy from the atomic and ionic states, where it is initially deposited, to the excimer states is based on the excited state structure of the rare gas dimers. This model was discussed in detail in our semiannual report[8] and is merely outlined here.

The $^1\Sigma_u^+$ and $^3\Sigma_u^+$ excimers are formed mainly by 3-body collisions of $^3P_1$ or $^3P_2$ atoms with ^1S ground state atoms. It can be shown that for Xe densities of 10^{21} cm^{-3} or less, higher order collision processes (e.g., 4-body collisions) are not important.

The energy deposition by high energy electrons (including the effect of secondaries) in rare gases produces mainly atomic ions. For example, in Ar, 78% of all excited particles are ions and 22% are excited atoms. For this reason, the electron-ion recombination is a major source of excited atoms when the excitation density is high enough. The dissociative recombination populates the band of np levels (4p in Ar, 6p in Xe) lying

just above the s levels from which the excimers are formed. Deactivation of the p levels to the s levels occurs by several mechanisms. At high pressures, formation of bound dimers, which predissociate either spontaneously or by collision with ground state atoms, is a major mechanism. At high electron densities, deactivation of both atomic and molecular excited levels by superelastic collisions can dominate the relaxation to the 4s levels and the excimer levels. Our reaction rate model is based on this simplified picture, which we believe includes the major formation and relaxation processes. The major uncertainty in the model centers on the role played by the electrons. In the high electron density cases required in the laser application, it is obvious that the electrons have a major effect on the deactivation. This effect is difficult to model realistically because cross sections of electron interaction with excited atoms and molecules are not known. We are, however, in the process of increasing the detail with which these interactions are treated in our model. The electron temperature is critically dependent on both excitation and deexcitation rates among the many close-lying excited levels. In the current modeling studies we have assumed the electron temperature to be constant at 1 eV for reasons presented in following sections. Again, we are in the process of including in the model a full calculation of the electron temperature, including energy dependent elastic and inelastic processes.

The reactions currently included in the model are summarized in Table II, together with our current best estimates of the corresponding reaction rates. These rates are based on direct measurements, or are estimates based on related measurements, as indicated by the listed references and discussed in our earlier report. Some rates have been modified slightly from our earlier estimates to provide better agreement of our modeling results with experiments. A similar model is being developed by George,[14] and preliminary results of this model have been reported.[15]

Modeling Calculations

The equations for the ionic and molecular formation, transfer, and decay processes summarized in Table II have been programmed for the computer.* Originally, the nonlinear differential equations were numerically integrated using a fourth-order Runga-Kutta procedure. Recently, however, we obtained an algorithm[16,17] designed especially for the integration of systems of "stiff" differential equations (i.e., the dependent variables are governed by rates that differ greatly in magnitude). This algorithm allows substantially larger integration step sizes than the Runga-Kutta method while retaining the required accuracy. (Treanor has described a similar procedure in some detail.[18]) The new integration package greatly reduces the computer time required for each case.

* The computer programming and calculations have been very ably carried out by Debasich Mukherjee.

TABLE II

REACTIONS AND RATES IN PURE XENON KINETIC MODEL

Reaction No.	Reaction	Rate (cm^3/sec, etc.)	Reference (see next page)
1	$Xe^+ + 2Xe \rightarrow Xe_2^+ + Xe$	2.5×10^{-31}	a, b, c, d
2	$Xe_2^- + e \rightarrow Xe^{**} + Xe$	2×10^{-7}	e
4	$Xe^{**} + 2Xe \rightarrow Xe_2^{**} + Xe$	10^{-31}	estimate
6	$Xe^{**} \rightarrow Xe^* + h\nu$	1.5×10^7	estimate, f
7	$Xe_2^{**} + Xe \rightarrow Xe^* + 2Xe$	10^{-11}	estimate
8	$Xe_2^{**} + e \rightarrow Xe_2^* + e$	10^{-6}	estimate
9	$Xe^* + 2Xe \rightarrow Xe_2^* + Xe$	5×10^{-32}	g, h
10	$Xe_2^* \rightarrow 2Xe + h\nu$	Variable	i
11	$Xe_2^* + e \rightarrow 2\,Xe + e$	10^{-9}	estimate, j
12	$Xe^{**} + Xe^{**} \rightarrow Xe^+ + Xe + e$	5×10^{-10}	j, k
13	$Xe_2^{**} + Xe_2^{**} \rightarrow Xe_2^+ + 2Xe + e$	5×10^{-10}	j, k
14	$Xe_2^* + Xe_2^* \rightarrow Xe_2^+ + 2Xe + e$	5×10^{-10}	j, k, l
17	$Xe^* + Xe^* \rightarrow Xe^+ + Xe + e$	5×10^{-10}	j, k

TABLE II (CONCLUDED)

REFERENCES

a. E. W. McDaniel, et al., Ion-Molecule Reactions (Wiley-Interscience, New York, 1970), p. 338.

b. D. Smith, A. G. Dean, and I. C. Plumb, J. Phys. B 5, 2134 (1972).

c. B. Mahan, J. Chem. Phys. 43, 3080 (1965).

d. A. P. Vitols and H. J. Oskam, Phys. Rev. A (to be published).

e. J. N. Bardsley and M. A. Biondi, in Advances in Atomic and Molecular Physics (Academic Press, New York, 1970), Chapter I.

f. Estimate based on corresponding transitions in argon. See W. L. Wiese, M. W. Smith, and B. M. Glennon, Atomic Transition Probabilities, Vol. II, NSRDS-NBS 4, 1966.

g. R. Boucique and P. Mortier, J. Phys. D 3, 1905 (1970).

h. This value is based on our analysis of the data of Koehler, et al., Phys. Rev. A (to be published).

i. See discussion in text, Section III.

j. D. C. Lorents and R. E. Olson, "Excimer Formation and Decay Processes in Rare Gases," Semiannual Report No. 1 Contract N00014-72-C-0457, Stanford Research Institute, December 1972.

k. Calculation based on theoretical arguments presented in Section IV.

l. J. B. Gerardo and A. W. Johnson, J. Chem. Phys. 59, 1738 (1973).

Sample calculations of the time-histories of several species concentrations in xenon pumped by a 3-nsec, 4-joule electron beam pulse are presented in Figures 3(a) through (g) for pressures from 0.27 to 41.5 atm (chosen to match data of Koehler et al.[6]). These calculations use a radiative time constant for Xe_2^* that is a function of pressure (this radiative time constant is discussed fully in a separate section). From Figures 3(a) through (g) we see that with the present model quite good agreement can be achieved between the predicted and measured concentration of Xe_2^*, although it should be noted that the pressure dependent lifetime has been obtained from experiment and that the experimental data have been normalized to the calculations at the maximum in each run because absolute measurements were not made.

Discussion of the Model

From a careful study of the computer-modeled results, we find that simple analytical relations can sometimes be used to predict species concentrations. For example, at the lowest pressure of 0.27 atm, we find that the Xe_2^* time decay is limited by its three-body production from Xe^* (i.e., excimer formation is the rate-limiting reaction). In the following analysis we also determine the radiative decay rate of Xe_2^*. Assuming an initial reservoir of atoms, $[Xe^*]_0$, the simplified equations become

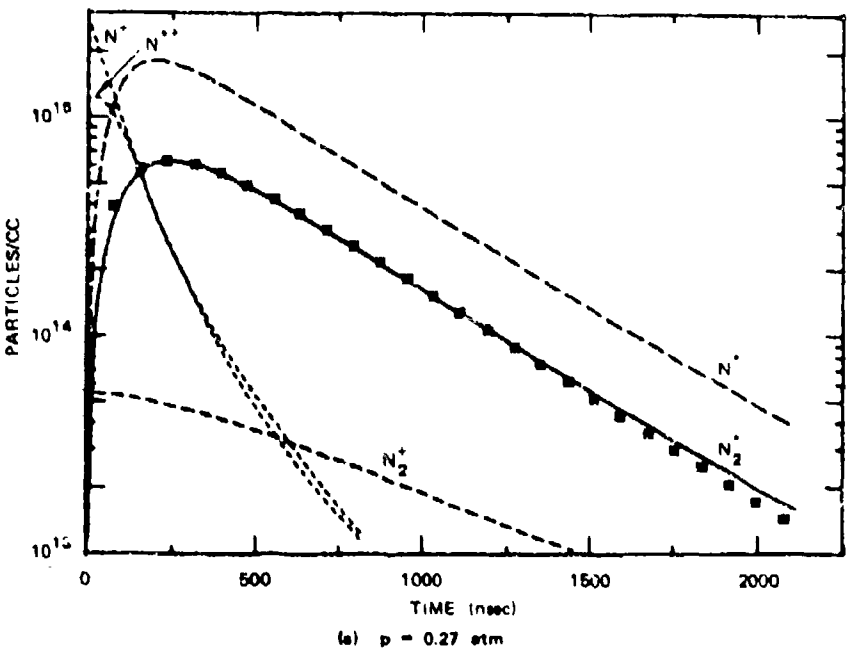

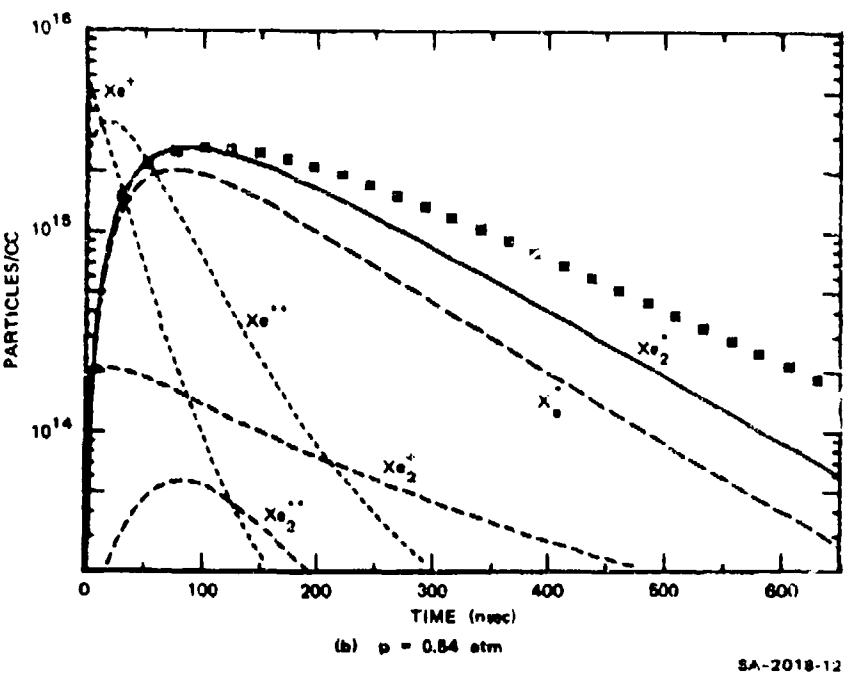

FIGURE 3 CALCULATED NUMBER DENSITIES OF VARIOUS SPECIES IN FEBETRON-EXCITED XENON

The points are from the intensity histories of Koehler, et al.[6], normalized to match the peak magnitude.

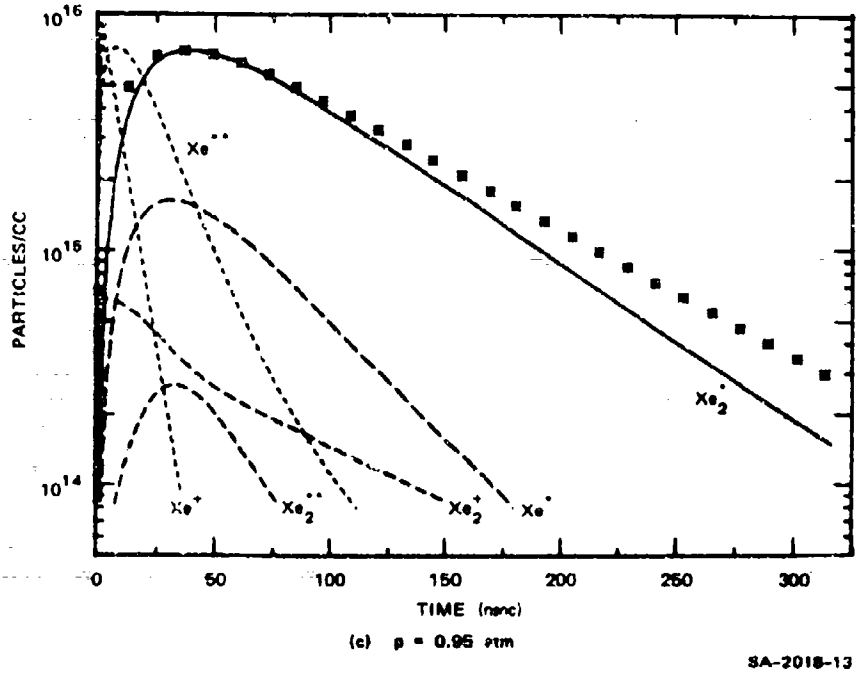

(c) p = 0.95 atm

SA-2018-13

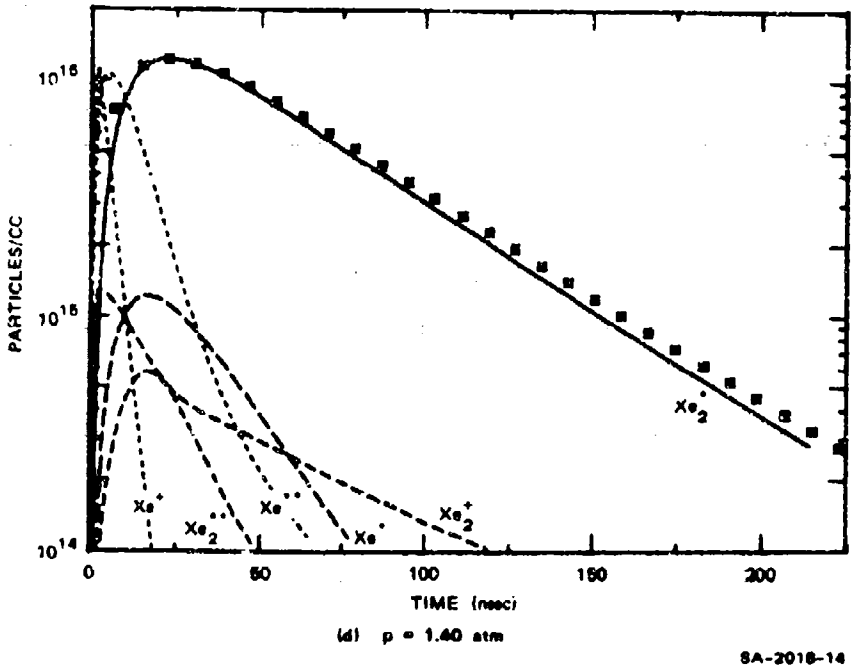

(d) p = 1.40 atm

SA-2018-14

FIGURE 3 CALCULATED NUMBER DENSITIES OF VARIOUS SPECIES IN FEBETRON-EXCITED XENON (Continued)

The points are from the intensity histories of Koehler, et al.[6], normalized to match the peak magnitude.

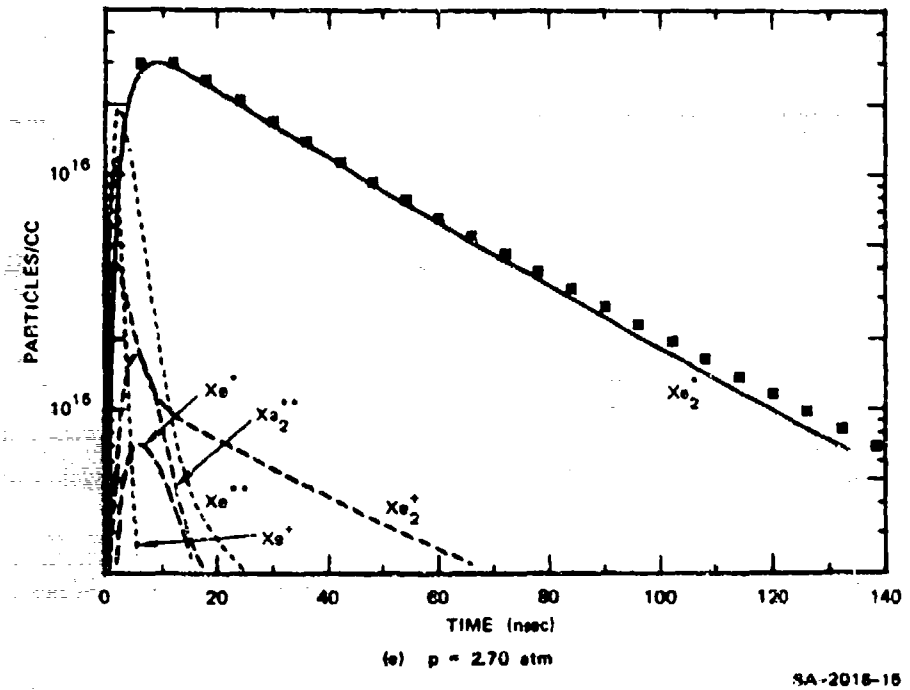

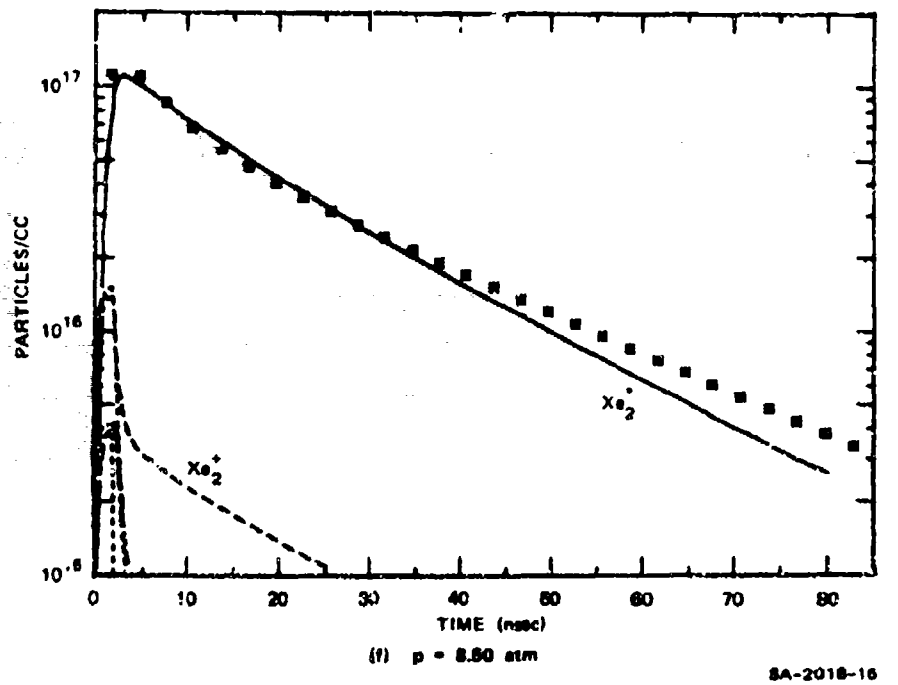

FIGURE 3 CALCULATED NUMBER DENSITIES OF VARIOUS SPECIES IN FEBETRON-EXCITED XENON (Continued)

The points are from the intensity histories of Koehler, et al.[6], normalized to match the peak magnitude.

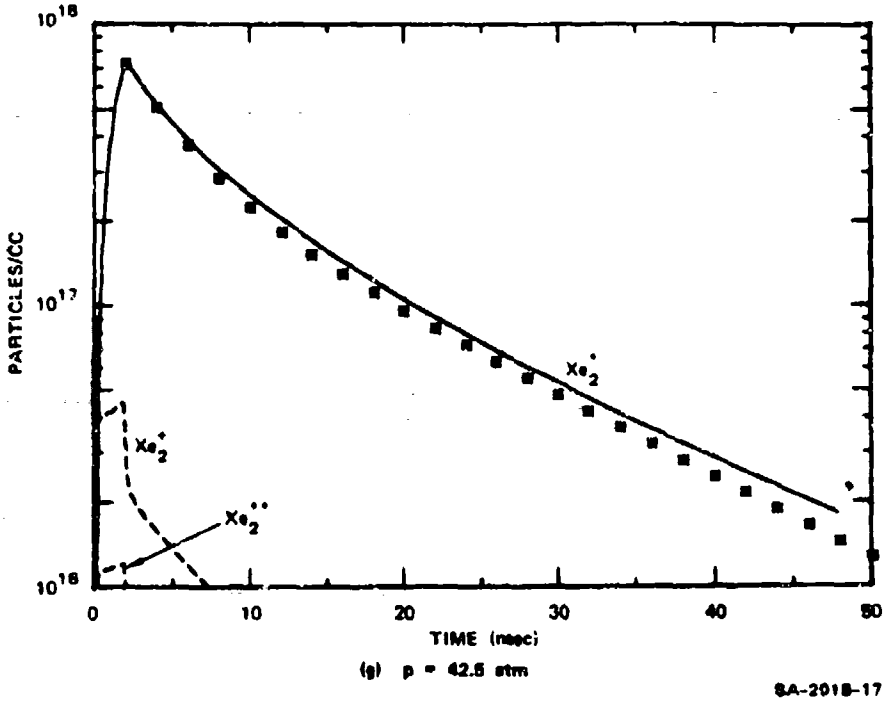

FIGURE 3 CALCULATED NUMBER DENSITIES OF VARIOUS SPECIES IN FEBETRON-EXCITED XENON (Concluded)

The points are from the intensity histories of Koehler, et al.[6], normalized to match the peak magnitude.

$$\frac{d[Xe^*]}{dt} = -k_9[Xe]^2\,[Xe^*] \tag{1}$$

and

$$\frac{d[Xe_2^*]}{dt} = k_9[Xe]^2\,[Xe^*] - k_{10}[Xe_2^*]\ , \tag{2}$$

where k_9 is the three-body association rate and k_{10} is the radiative decay rate. These equations have the solution

$$[Xe^*] = [Xe^*]_o \exp\{-k_9[Xe]^2\,t\} \tag{3}$$

$$[Xe_2^*] = \frac{k_9[Xe^*]_0\,[Xe]^2}{k_{10} - k_9[Xe]^2}\left(\exp\{-k_9[Xe]^2 t\} - \exp[-k_{10}t]\right)\ . \tag{4}$$

If $k_{10} \gg k_9[Xe]^2$, then the long-time decay rate is $k_9[Xe]^2$, and the experimental results show just this result. Under these conditions, the reactions expressed in equation (2) are in quasi-steady state; thus the magnitude of $[Xe_2^*]$ is related to $[Xe^*]$ by

$$\frac{[Xe_2^*]}{[Xe^*]} = \frac{k_9[Xe]^2}{k_{10}} \tag{5}$$

This constant ratio of populations is shown in Figure 3(a).

Finally, from the derivative of equation (3), the maximum $[Xe_2^*]$ concentration occurs at a time where

$$k_{10}\exp\{-k_{10}t\} = k_9[Xe]^2\exp[-k_9[Xe]^2 t]\ . \tag{6}$$

Since the maximum is observed to occur at approximately 240 nsec [Figure 3(a)] we can solve this implicit equation to find that $k_{10} = 6 \times 10^6$ at these conditions. Taking into account the fact that $[Xe^*]$ is not simply decaying exponentially at the early times makes k_{10} somewhat larger. The computer results shown in Figure 3(a) were generated assuming $k_{10} = 9 \times 10^6$, and indeed the agreement between the predicted and measured $[Xe_2^*]$ history is excellent. This lifetime of 110 nsec we believe is that of the $^3\Sigma_u^+$ level.

For high pressures, similar considerations can be applied to the electron density and electron temperature at times after the atomic ion concentration has decayed. Then electrons and molecular ions are produced only by the Penning ionization process [primarily reaction (14), Table II] and are removed by the recombination reaction (2), Table II. The rate equation for electrons under these conditions (note that $n_e \cong [Xe_2^+]$) is

$$\frac{dn_e}{dt} = k_{14}[Xe_2^*]^2 - k_2[n_e]^2 . \qquad (7)$$

Again, a quasi-steady state exists during the decay, and the electron density is related to the excimer concentration by

$$\frac{n_e}{[Xe_2^*]} = \left(\frac{k_{14}}{k_2}\right)^{\frac{1}{2}} \qquad (8)$$

The constant ratio of n_e to $[Xe_2^*]$ is clearly shown in Figures 3(e) through 3(g).

The electron temperature is governed by a combination of several processes: heating from the Penning electrons [reaction (14), Table II], superelastic collisions, energy loss when electrons recombine [reaction (2), Table II], and cooling by elastic and inelastic collisions. Neglecting the effects of superelastic and inelastic collisions for this discussion, the differential equation for the electron temperature is

$$\frac{dT_e}{dt} = \frac{1}{n_e}\left\{k_{14}[Xe_2^*]^2\,[3.3 - T_e] - K_e \cdot N \cdot n_e \cdot T_e\right\} \text{ eV/sec} , \qquad (9)$$

where K_e is the rate constant for elastic cooling and the electron emitted in the Penning ionization has 3.3 eV energy. If we again assume quasi-steady state and use equation (8) above, then the electron temperature is

$$T_e \simeq \frac{3.3}{1 + K_e N/\{[Xe_2^*](k_{14}k_2)^{\frac{1}{2}}\}} . \qquad (10)$$

The ratio of rates has the approximate value $K_e/(k_{14}k_2)^{\frac{1}{2}} \sim 10^{-5}$ (valid for $0.2 < T_e < 1$ eV). Therefore, for the degree of excitation ($[Xe_2^*]/N$) predicted for Febetron experiments, equation (10) indicates that the electron temperature will vary as the excimers decay.

It should be noted that the rate constant for elastic cooling increases precipitously for electron temperatures above 1 eV, by as much as a factor of 100 at 2 eV. Furthermore, inelastic collisions begin to

be significant above 1 eV. These two effects counteract the rather high electron temperature predicted by equation (10), and should maintain the electron temperature at between 1 and 1.5 eV. At these electron temperatures, electrons play an important role in mixing electronic states of both atoms and excimers. This electron mixing is not satisfactorily accounted for in our present kinetic model. The implications of the electron mixing on excimer radiative lifetime are discussion in Section III.

III RADIATIVE LIFETIMES OF RARE-GAS EXCIMERS

One of the fundamental parameters in any laser system is the radiative lifetime of the upper laser level. In the case of the rare gas dissociation lasers being considered here, both experimental and analytical efforts thus far have taken the simple approach of considering one excimer state with single lifetime, whereas the state structure clearly indicates that there are two radiating levels. Measurements of intensity decays of the excimers following pulsed excitation are difficult to interpret on the basis of a single lifetime, however, because results using high electron density pumping differ markedly from those using low electron density pumping, even at the same pressure, and because the radiative decay rate in the high electron density studies is pressure dependent. Quenching of excimers to the ground state has been advanced as an explanation of the latter effect.

In this section, we consider in detail the contribution of two excimer states to the observed radiation. These states have markedly different radiative lifetimes, and taking proper account of the collisional mixing of the states may furnish an explanation for the observed radiative decay in all the experiments. After examining the experimental and theoretical aspects of this lifetime problem, we conclude that the decay lifetimes observed in the high density excitation case are dominated by electron induced mixing of the states.

Status of Experiments

Measurements yielding information on the radiative decay of rare gas excimers can be divided into two groups. One group includes measurements at low pressures (< 1 atm) with excitation by very low current beams of charged particles (either electrons or protons).[19-22] These studies indicate the existence of pressure-indpendent decay constants ranging in magnitude from 0.3 to 5 μsec for Xe_2^*, Kr_2^*, Ar_2^*, and Ne_2^* (see Table III, p. 31). The second group includes measurements at higher pressures (up to 50 atm) obtained with high current pulsed electron beam excitation (Febetron 706).[1,6,23-25]

There is, unfortunately, strong disagreement among the various experimentalists on how to interpret and analyze these high-pressure data. The problem is complicated by the fact that the excimer decay results both from the radiative decay from two states with different lifetimes and from an excimer-excimer collisional deactivation (Penning ionization), as expressed by the rate equation

$$\frac{d[N_2^*]}{dt} = -k_{14}[N_2^*]^2 - k_{10}[N_2^*], \qquad (11)$$

where $[N_2^*]$ is the sum of the concentrations of the two excimer states, k_{14} is the excimer-excimer rate, and k_{10} is a weighted combination of the two radiative decay rates (the treatment of the decay of the two states as separate entities is discussed below). When the excimer concentration

is high (at early times in the decay and typically at high pressure, since energy deposition in the gas increases with increasing pressure), the early time decay of excimer radiation can be dominated by the excimer-excimer process. We believe this effect is clearly shown in the results presented by Koehler et al.[1,6] In subsequent papers, Wallace et al.[24] describe the decay of xenon in terms of early and late time constants, and Koehler et al.[6] find it necessary to fit the decay of both argon and xenon with the sum of several exponential terms. Bradley et al.[23] do not distinguish two time constants, but we believe that they also report an early time decay rate that is governed by excimer-excimer processes.

On the other hand, Gerardo and Johnson[25] have analyzed their measurements of the xenon decay according to equation (1) and have determined the exponential component of the decay rate. We have reconstructed the xenon data of Koehler et al. from their curve fit parameters and have analyzed these data in terms of equation (1) to extract an exponential decay rate. We have also analyzed the few intensity histories presented in references (23) and (24) and determined such a rate. All these results are presented in Figure 4. The various measurements are in reasonable agreement with each other, and the exponential decay rate is pressure dependent! At high densities, however, the decay rate reaches an asymptotic value. Unfortunately, only the Livermore results extend to sufficiently high densities to show this

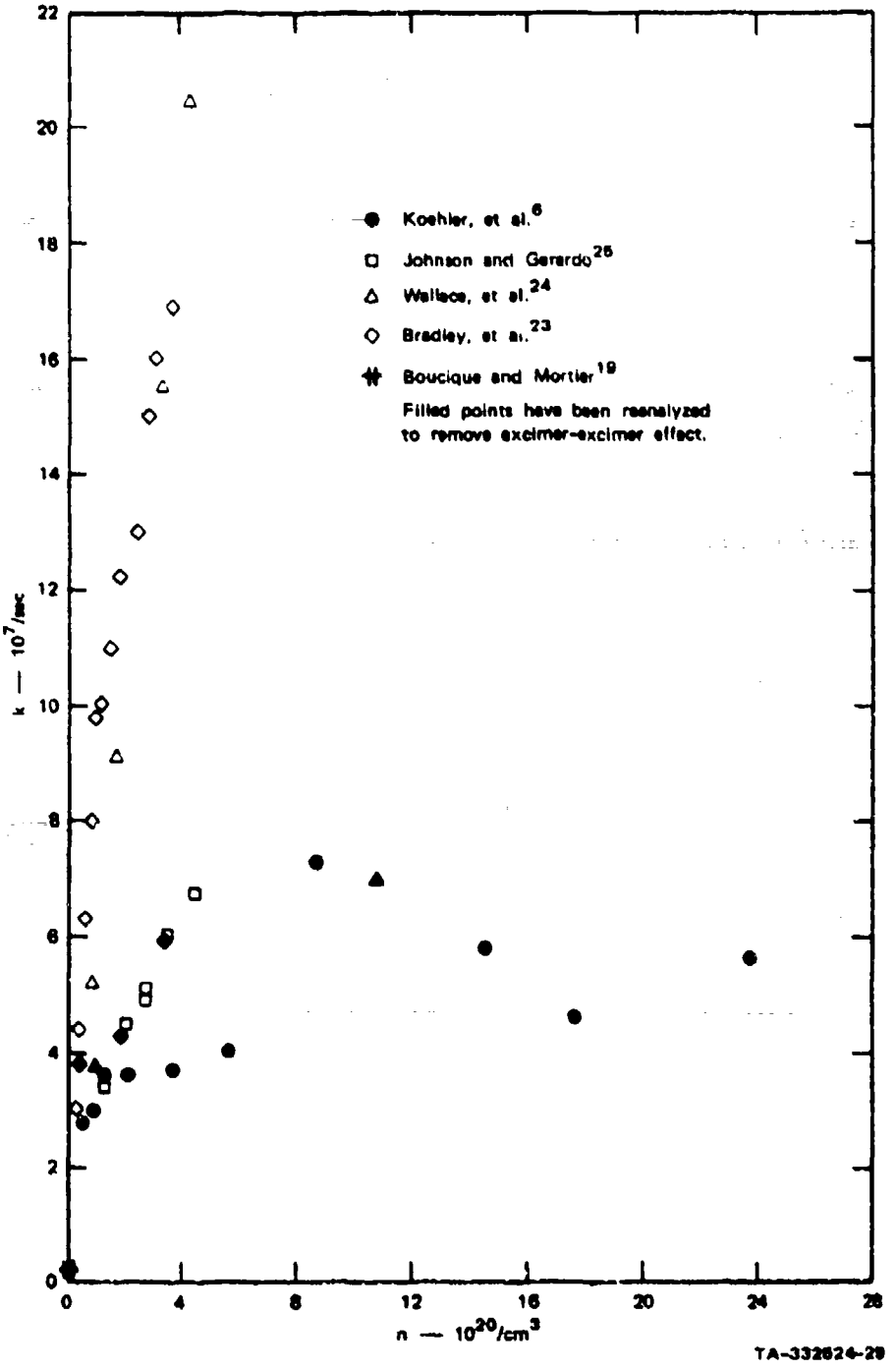

FIGURE 4 SUMMARY OF MEASUREMENTS OF THE RADIATIVE DECAY RATE OF THE XENON EXCIMER

effect. This point is fundamental to the interpretation of the pressure dependence; if it is due to a two-body collisional quenching of excimers to the ground state, the decay rate will be linear in number density at all pressures, and extrapolation to zero pressure gives the radiative lifetime. The existence of an asymptote, on the other hand, implies a collisional mixing of two states with differing lifetimes (e.g., $^3\Sigma_u^+ + {}^1\Sigma_u^+$). The pressure dependence of the decay rate in this case is discussed in the next subsection. Because of the importance of a correct interpretation of the decay rate, we hope that all the data reported in references (23) and (24) can be reanalyzed to determine the pure exponential decay rate for comparison with the values presented in Figure 4.

The various interpretations of the decay rates, and their extrapolation to zero pressure, have resulted in estimations of excimer radiative lifetimes for Xe_2^* ranging from 16 to 130 nsec. The data of Koehler et al.[6] indicate that the decay rates of argon are similar to those of xenon. These results should be compared with the pressure-independent decay rates of 500 nsec for xenon[19] and 2.8 and 3.7 μsec for argon[19,20] obtained at low excitation density.

The lifetime data of Koehler et al. extends to pressures as low as 0.27 atm. The trend of the data is toward progressively longer lifetimes with decreasing pressure below 1 atm. Our kinetic modeling results show that at these low densities the molecular excimer production becomes rate-limiting.

Theoretical Predictions of Excimer Lifetimes

The 1_u sublevel of the $^3\Sigma_u^+$ excimer state derives most of its transition strength to the ground $^1\Sigma_g^+$ state by spin-orbit mixing with the $^1\Pi_{1u}$ state. This mixing is represented by

$$|1_u\rangle = C_1|^3P_2^1\rangle + C_2|^3P_1^1\rangle + C_3|^1P_1^1\rangle \quad . \tag{12}$$

The $^3\Sigma_u^+$ state dissociates to $^3P_2$ at internuclear distance $R = \infty$; hence, at very large R the coefficients have the values $C_1 \sim 1$, $C_2 \sim C_3 \sim 0$. At finite internuclear distances, including the equilibrium distance R_e, C_3 is nonzero, and its value can be found by diagonalizing the 1_u Hamiltonian in Table I. This leads to the relations

$$\tfrac{1}{2}\zeta C_2 + \left(\frac{W}{2} + G - \lambda\right) C_3 = 0 \ , \tag{13}$$

$$\left(\frac{\zeta}{2} - G - \lambda\right) C_1 - \frac{W}{2} C_2 = 0 \ , \tag{14}$$

and

$$C_1^2 + C_2^2 + C_3^2 = 1 \ , \tag{15}$$

where λ is the energy of the $^3\Sigma_{1u}^+$ state.

Assigning a transition strength of 1 to the pure $^1P_1$ state, we can define the transition strength of the $^3\Sigma_{1u}^+$ state by

$$C_3^2 = \left\{1 + \left(\frac{W/2 + G - \lambda_{1u}}{\sqrt{2}\zeta}\right)^2 \left[1 + \left(\frac{W/2}{\zeta\sqrt{2} - G - \lambda_{1u}}\right)^2\right]\right\}^{-1} . \quad (16)$$

Similarly the transition strength of the $^1\Sigma_{0u}^+$ state would be

$$\left\{1 + \left(\frac{-W/2 + G - \lambda_{0u}^+}{\sqrt{2}\zeta}\right)^2\right\}^{-1} . \quad (17)$$

Calculations of the relative lifetimes of the singlet and triplet excimer states can now be made insofar as we know the values of the parameters appearing in the above equations. The values of ζ and G are known from atomic parameters, as discussed in Section II. The value of W depends on the Σ-Π splitting at R_e, which is unknown but can be calculated from the excimer binding energies. We discussed estimates of the binding energies of Ar_2^* and Xe_2^* in Section II; values for Ne, Ar, Kr, and Xe are all believed to be in the range from 0.5 to 1 eV. This corresponds to Σ-Π splittings of 8000 to 16000 cm^{-1}.

The results of calculations of the ratio of triplet (1_u) to singlet (0_u^+) lifetimes are presented in Tablo III for binding energies of 0.5 and 1 eV. The range of triplet lifetimes is also given, under the assumption that the (0_u^+) lifetime is about the same as the corresponding atomic state, namely, 4 nsec. Lifetimes of the rare gas excimers that have been observed in various experiments using low electron density pumping are shown for comparison (we implicitly assume here that the decay rate in these experiments is the triplet excimer lifetime).

TABLE III

ESTIMATED LIFETIMES OF TRIPLET EXCIMERS

Excimer	τ_{1u}/τ_{0u}^{+}		τ_{1u}	Experimental Values
	D_e = 0.5 eV	D_e = 1.0	if τ_{0u}^{+} = 4 nsec	
Ne_2^*	1460.	4800	5.8 - 19 μsec	5.1 μsec[a]
Ar_2^*	470	1500	1.9 - 6 μsec	2.8 μsec,[b] 3.7 μsec[c]
Kr_2^*	48	130	0.19 - 0.52 μsec	0.3 μsec,[d] 1.7 μsec[c]
Xe_2^*	24	46	96 - 184 nsec	100-160 nsec,[e] 500 nsec[c]

[a] P. K. Leichner, Phys. Rev. A 8, 815 (1973).

[b] N. Thonnard and G. S. Hurst, Phys. Rev. A 5, 1110 (1972).

[c] R. Boucique and P. Mortier, J. Phys. D. 3, 1905 (1970).

[d] P. K. Leichner and R. J. Ericson, Phys. Rev. A (in press).

[e] From analysis of data of Koehler, et al.[6] at 0.27 atm.

The measured values fall within or near the range of predicted values, except for the 1.7-μsec value for Kr_2^* and the 500-nsec value for Xe_2^*. The good agreement in the other cases may indicate that the two noted values may represent the radiative lifetime of some excimer state other than the lowest triplet state.

Effect of Two Lifetimes on Observed Radiative Decay

In subsections above, we have described experiments that indicate radiative lifetimes for Ar_2^* and Xe_2^* that differ by as much as two orders of magnitude, depending on the experimental conditions. We have also indicated the existence of two closely spaced excimer states, one a triplet and one a singlet, and have predicted their relative radiative lifetimes. In following paragraphs, we discuss how the existence of two radiative lifetimes influences the observed radiative decay.

For convenience, we will orient our discussion toward Xe, although it applies to the other rare gases as well. For Xe, we estimate that the fully allowed transition from the singlet excimer to the ground state has a radiative lifetime of approximately 4 nsec, while the triplet lifetime should be in the range 100 to 200 nsec. We have already indicated that the 500 nsec lifetime measured by Boucique and Mortier[19] is probably not the triplet lifetime. On the other hand, the Febetron experiments show radiative decay rates that vary with pressure in the range from 10 to 100 nsec. In seeking to explain the observed results,

we examine the interplay of two radiating states and collisional effects, including quenching to the ground state by atoms and mixing of the two states by atoms and by electrons. We finally conclude that electron mixing dominates.

The rate equations for decay of two molecular states (neglecting initial formation processes) are:

$$\frac{dN_1}{dt} = -\left\{k_{R_1} + \left[k_{Q_1} + k_{d_a}\right] N_a + k_{d_e} N_e\right\} N_1 + \left\{k_{u_a} N_a + k_{u_e} N_e\right\} N_3 \tag{18}$$

and

$$\frac{dN_3}{dt} = -\left\{k_{R_3} + \left[k_{Q_3} + k_{u_a}\right] N_a + k_{u_e} N_e\right\} N_3 + \left\{k_{d_a} N_a + k_{d_e} N_e\right\} N_1 \quad , \tag{19}$$

where N is population and the subscripts 1, 3, a, and e refer to singlets, triplets, ground-state atoms, and electrons, respectively. The subscripts R, Q, u, and d on the rates refer to radiation, quenching to the ground state, and upward and downward mixing between the two states by atoms and electrons. The solution to these equations has the form

$$N_1 = C_{11} e^{\lambda_1 t} + C_{12} e^{\lambda_2 t} \tag{20}$$

and

$$N_3 = C_{21} e^{\lambda_1 t} + C_{22} e^{\lambda_2 t} \quad , \tag{21}$$

where the exponential time constants are

$$\lambda_{1,2} = -\tfrac{1}{2}\left(k_{R_1} + k_{R_3} + \left[k_{Q_1} + k_{Q_3} + k_{d_a} + k_{u_a}\right]N_a + \left[k_{u_e} + k_{d_e}\right]N_e \right)$$

$$\pm\tfrac{1}{2}\left(\left\{k_{R_3} - k_{R_1} + \left[k_{Q_3} - k_{Q_1} + k_{u_a} - k_{d_a}\right]N_a + \left[k_{u_e} - k_{d_e}\right]N_e\right\}^2\right.$$

$$\left. + 4\left[k_{u_a}N_a + k_{u_e}N_e\right]\left[k_{d_a}N_a + k_{d_e}N_e\right]\right)^{\frac{1}{2}} \qquad (22)$$

We can now examine these time constants under a variety of assumptions.

At low N_a and N_e, the time constants simplify to

$$\lambda_{1,2} \rightarrow -k_{R_1}, -k_{R_3} \quad , \qquad (23)$$

which implies no quenching and no mixing, and each state decays with its own radiative lifetime. If $k_{R_1} \gg k_{R_3}$, the faster component of radiation may be masked by the excimer formation time, and the only lifetime observed will correspond to k_{R_3}. This is the justification for identifying the 100-160 nsec decay constant observed in the low pressure Livermore data as the triplet lifetime for Xe_2. Similarly, for Kr_2, Leichner and Ericson obtained 300 nsec; and in Ar, Thonnard and Hurst found a lifetime of 2.8 μsec comparable to Boucique and Mortier's 3.7 μsec lifetime (Table III).

Now let us consider the effects of quenching to the ground state. If we neglect k_u and k_d, the solutions become

$$\lambda_1 = -\left(k_{R_1} + k_{Q_1} N_a\right), \tag{24}$$

$$\lambda_2 = -\left(k_{R_3} + k_{Q_3} N_a\right). \tag{25}$$

With these assumptions, the decay rates must increase linearly with density at all densities! In those experiments where the pressure dependence of the radiative decay is attributed to quenching,[23-25] the rate k_Q is found to vary in the range $(0.9 \rightarrow 5) \times 10^{-13}$ cm^3/sec. There are two arguments against this interpretation, however. First, Boucique and Mortier observed a 500 nsec radiative decay from an excimer state of Xe_2 that was independent of pressure up to 460 torr. This indicates that $k_Q N \ll k_R$, or $k_Q \ll 10^{-13}$ cm^3/sec. The second, and more important, argument is a theoretical one. Since there are no potential curve crossings between the ground $^1\Sigma_g^+$ and the excimer states and since the separation between these states is so large, collision-induced transitions at thermal energies should be completely negligible. These states are analogous to the $N_2(A^3\Sigma_u^+)$ state, which is quenched by argon at a rate less than 10^{-17} cm^3/sec, and by xenon at less than 2×10^{-16} cm^3/sec (ref. 26).

Let us now consider the mixing of singlet and triplet populations by atomic collisions (neglecting quenching and mixing by electrons for the moment). The exponential decay rates are

$$\lambda_{1,2} = -\tfrac{1}{2}\left\{k_{R_1} + k_{R_3} + \left[k_{d_a} + k_{u_a}\right]N_a\right\}$$

$$\pm\tfrac{1}{2}\left(\left\{k_{R_3} - k_{R_1} + \left[k_{u_a} - k_{d_a}\right]N_a\right\}^2 + 4k_{u_a}k_{d_a}N_a^2\right)^{\frac{1}{2}} . \qquad (26)$$

This result displays the features of the experimentally observed decay rates. In particular the smaller of the rates λ_2 (i.e., the longer, observed decay time) is density dependent, with the limiting values $\lambda_2 \to -k_{R_3}$ as $N_a \to 0$ and

$$\lambda_2 \cong -k_{R_3} - \frac{\left[k_{R_1} - k_{R_3}\right]k_{u_a}N_a}{\left[k_{R_1} - k_{R_3}\right] + \left[k_{d_a} + k_{u_a}\right]N_a} \qquad (27)$$

$$\cong -k_{R_3}\left[\frac{1}{1 + K_c}\right] - k_{R_1}\left[\frac{K_c}{1 + K_c}\right]$$

as $N_a \to \infty$, where $K_c = k_u/k_d$ is the equilibrium constant,

$$K_c = \frac{g_1}{g_3}\exp\left[-(E_1 - E_3)/kT_a\right] \qquad (29)$$

$$\cong \frac{1}{3}\exp\left[-1000/T_a\right] \qquad (30)$$

Note that both the singlet and triplet excimers decay with a common rate that is a weighted mixture of their radiative decay constants.

We have replotted the experimentally observed decay constants (after correction for excimer-excimer effects) in Figure 5, and have also plotted the solution of equation (26) for a set of parameters that gives agreement with the data. Note that the choice of $k_{R_1} = 1.3 \times 10^9$ sec^{-1} is dictated by equations (28) and (30) together with the assumed asymptote of the data at $k = 6 \times 10^{+7}$ sec^{-1}. Furthermore, we set $k_{R_3} = 2 \times 10^6$ sec^{-1} as discussed above, so that the only free parameter is k_{d_a}. As seen from Figure 5, the fit of the curve to the Febetron experimental data is quite appealing. Unfortunately, there are two problems. The first is the value of k_{R_1} that must be used to give the correct asymptotic value. It corresponds to a singlet radiative lifetime of 0.8 nsec and is too short to believe (the corresponding atomic state has a lifetime of 4 nsec). The value of k_{R_1} does depend on K_c, which in turn depends on the gas temperature as indicated by equation (29). We have taken $T \leq 500^{\circ}K$ based on calculations of the total energy deposited in the Febetron experiments. The temperature would have to be substantially higher for k_{R_1} to become a reasonable value. Also, the value of k_{R_1} required to give the correct asymptotic value is only weakly dependent on k_{R_3}. For example, if the triplet radiative rate is near the predicted value of 10^7 sec^{-1} rather than 2×10^6 sec^{-1} as observed by Boucique and Mortier, then the value of k_{R_1} is reduced only to 1.2×10^9. This is still not a reasonable value.

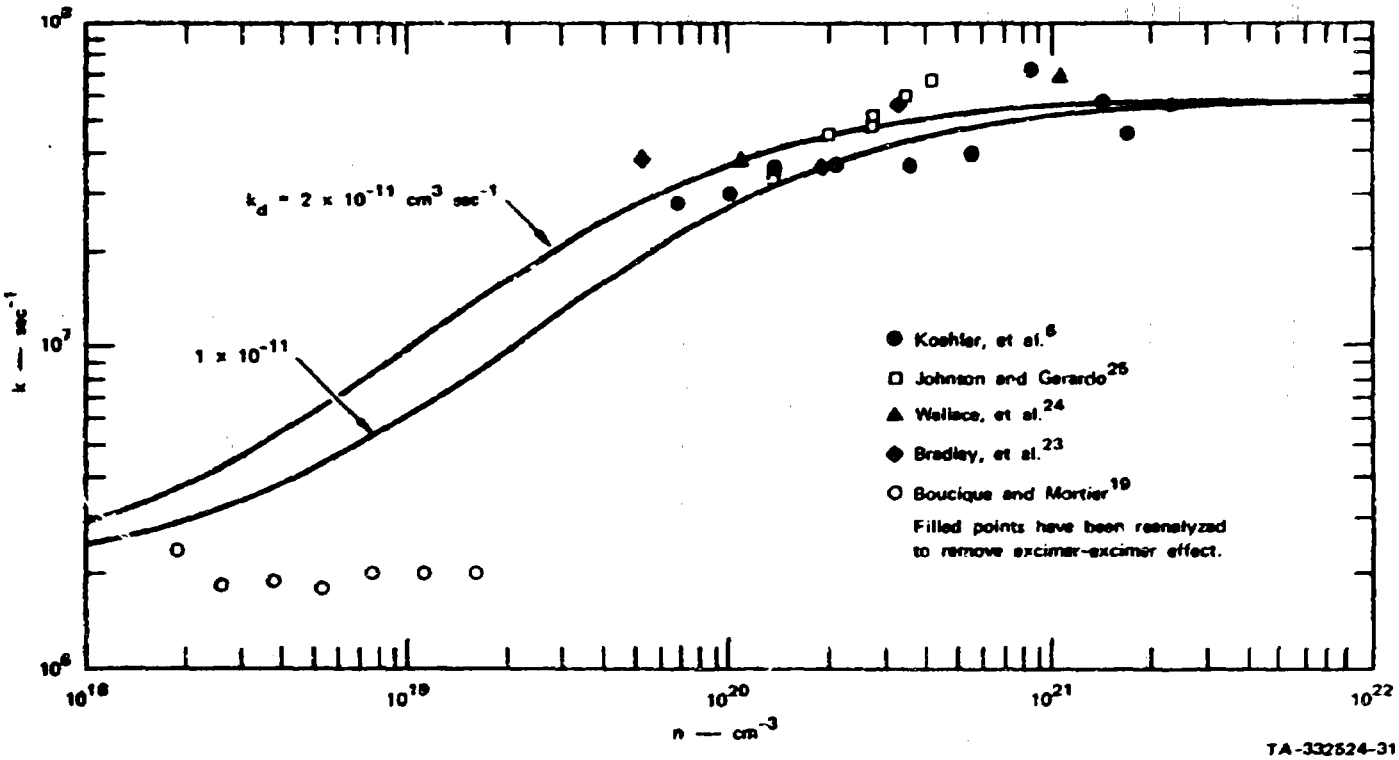

FIGURE 5 COMPARISON OF EXPERIMENTAL XENON RELAXATION RATES WITH TWO-STATE MODEL USING MIXING BY ATOMS [k_{R_3} = 2 x 10^6 sec^{-1}, k_{R_1} = 1.3 x 10^9, K_c = 0.045 (T_{gas} = 400°K)]

The shortcomings of the explanation outlined above, and the fact that the lifetime data generally fall into categories of either quite low or quite high electron densities lead us to consider, finally, the mixing of populations of the singlet and triplet states by electrons. The rates given by equations (27) through (30) pertain in this case also, but with the subscript a replaced by e, and we see that the lifetime is a function of both electron density and electron temperature. Thus it is possible to have different lifetimes at the same gas density. This would explain not only the differences between the high and low electron density data, but may also explain the smaller differences among the Febetron results as noted most clearly in Figure 4. That is, what appears to be a pressure-dependent radiative lifetime could in fact be an electron-dependent lifetime, with differences between various experiments reflecting different electron-beam pumping rates, viewing of different geometric areas in the gas, and so on.

On first consideration, it would appear that the dependence of the lifetime on electron density and temperature would in fact cause the lifetime to vary with time following the electron pulse, as both electron density and temperature decay. However, in the Febetron experiments the electron density is generally high enough throughout the decay to make the lifetime take its high-density asymptotic value for the observation period. Referring to equations (27) and (28), we see

that the decay rate takes on its asymptotic value when

$$k_{u_e} \cdot (1 + 1/K_c)N_e \gg (k_{R_1} - k_{R_3}) \quad . \tag{31}$$

We estimate that $k_{u_e} \simeq 10^{-6}$ cm^3/sec and $K_c \leq 0.33$. If we take as an upper limit $k_{R_1} = 2 \times 10^8$ sec^{-1}, then we find that relation (31) holds when $N_e \gg 5 \times 10^{13}$. Our modeling calculations show that this inequality holds, for all but the lowest pressures, throughout the decay for the Febetron experiments. We then conclude that the "pressure dependence" observed in the Febetron experiments is related to the electron temperature T_e.

The electron temperature during the decay was discussed in Section II. It was noted that a high excimer concentrations the Penning ionization of excimers tends to drive T_e up toward 3.3 eV, but that the rapid increase of both elastic and inelastic cooling rates for energies about 1 eV will counteract the ionization heating and tend to keep T_e near 1 eV. Then the asymptotic decay rate has the values (for $k_{R_3} = 10^7$ sec^{-1})

T_e (eV)	$k_{asymptotic}$ (sec^{-1})
0.4	4.99×10^7
0.7	5.32×10^7
1.0	5.44×10^7
1.3	5.51×10^7
1.6	5.54×10^7

Thus, the variation of the decay rate is not very large for this range of electron temperatures, and the magnitude agrees well with the values observed in the Febetron experiments for pressures above 1 atm. It remains to be seen whether a reasonable variation with pressure can be predicted or if the decay rate will be as nearly constant with time throughout the decay as the experimental results indicate. We are currently modifying our kinetic modeling computer program so that we can study this in detail. It certainly seems, however, that mixing of the two states by electrons is an important process in determining the observed excimer decays.

IV LOSS MECHANISMS

Several important excimer loss mechanisms exist that under certain conditions can reduce the efficiency for spontaneous radiation and for lasing. These include collisional quenching by ground state atoms, excimer-excimer collisional deactivation, and photoabsorption by photoionization of excimer states or by absorption from transient ground state dimers. Our earlier analysis of the energy deposition indicated that an upper limit to the efficiency of producing excimers is about 50%. This will be reduced further if any of the above processes are important. Measurements of the efficiency have been reported ranging from 10 to 30%. The photoabsorption processes are particularly important for the laser because they reduce the gain as well as the efficiency.

Collisional Losses

Quenching of the excimers to the ground state by ground state atoms has been advanced as the explanation of the linear pressure dependence observed in some experiments,[23-25] and in these cases rate constants on the order of 10^{-13} cm^3/sec have been reported. As discussed in the previous section, we believe that the pressure dependence is due instead to collisional mixing (mainly by electrons) of the singlet and triplet populations. Quenching of the excimers

to the ground state by ground state atoms is extremely slow because of the large separation in energy between the ground $^1\Sigma$ and and the excited $^3\Sigma$ at all internuclear separations. An extremely hard collision is required to distort the excimer state enough to permit a non-radiative transition to the ground state. An example of a system that has a similar ground state-excited state separation is $N_2(A)$ in N_2. In this case the quenching rate constant is less than 10^{-17} cm^3/sec.[26]

A more important quenching mechanism that occurs at high excitation densities is that of excimer-excimer collisions. This is a Penning ionization process in which one electron is ejected, absorbing the excess reaction energy, and one excimer is deactivated. The rate constant for this kind of process has been measured for $He(2^3S)$ + $He(2^3S)$ to be 4×10^{-9} cm^3/sec.[27] Since the ionization potentials of Xe_2^* and of $He(2^3S)$ are nearly the same, we expect the reaction cross sections to be similar, so that the rate constant simply scales with velocity. On this basis we estimate the rate constant to be approximately $k_{14} = 8 \times 10^{-10}$ cm^3/sec; this should be a lower limit since the Xe excimer should be physically larger than $He(2^3S)$. In the calculations reported here, the value of $k_{14} = 5 \times 10^{-10}$ cm^3/sec was used, but the fit to the data would be improved if k_{14} were increased to 1.0×10^{-9} cm^3/sec.

Gerardo and Johnson obtained the quantity $k_{14}[Xe_2^*]_o$ from an

analysis of their data.[25] Using their 50-nsec radiative lifetime, they determined $[Xe_2^*]$ from absolute intensity measurements, and determined k_{14} to be 3.5×10^{-10} cm^3/sec. However, if one uses the 16-nsec lifetime, which we believe is correct for the high electron density case, then $k_{14} \cong 10^{-9}$ cm^3/sec, in good agreement with the theoretical estimate.

Photoionization

The quantum defect method[28] has been used for some years in the calculation of photoionization cross sections. The quantum defect itself enters in two ways. First, it describes the size of the orbital occupied by the electron before photoionization, thus setting the general scale of the problem. Second, the quantum defect describes the phase shift of the final state coulomb wave. The value of the dipole matrix element $(\Phi_{final}|\vec{r}|\Phi_{initial})$ can be quite sensitive to this phase shift. This effect is the reason for the small magnitude of the threshold photoionization cross sections of the alkali atoms. The effect is washed out at higher photon energies.

In estimating the cross sections for photoionization of the rare gas excimers, we make the simple assumption that the phase shift of the final state is not important. The effects to be included are the ionization potential (i.e., quantum defect) and the decrease of the dipole matrix element due to rapid oscillation of the final state as the impact energy is increased. Specifically, we follow the method of Bethe and Salpeter,[29] who give the formula (for a hydrogen atom)

$$\frac{dF_n}{dv'} \approx \frac{1.96}{v'^3 n^3}$$

to describe the oscillator strength, F_n, per unit of relative frequency, summed over all $2n^2$ sublevels with principal quantum number n, where $v' = \frac{h\nu}{Z^2 Ry}$, $n^2 = \frac{Z^2 Ry}{IP}$, Z is the ionic charge after photoionization, $h\nu$ is the photon energy E, Ry is the Rydberg unit of 13.6 ev, and IP is the ionization potential. The total oscillator strength per unit energy is then

$$\frac{dF_n}{dE} = \frac{1.96\ ZRy^{\frac{1}{2}}}{IP^{\frac{1}{2}}\rho^3} \qquad (33)$$

where ρ is the relative energy E/IP. The average oscillator strength, f_n, can be found by dividing by the number of electrons that could be put in the n^{th} shell, which is $2n^2$ (since each sublevel could be doubly occupied), to give

$$\frac{df_n}{dE} = \frac{0.98}{ZRy^{\frac{1}{2}} IP^{\frac{1}{2}} \rho^3} \qquad (34)$$

Finally we can calculate the photoionization cross section[30] <u>per electron</u> as

$$\sigma = 0.807 \times 10^{-17} \frac{df}{dE} \quad (cm^2) \qquad (35)$$

or

$$\sigma = \frac{8 \times 10^{-18}}{Z(IP/13.6)^{\frac{1}{2}}\rho^3} \quad (cm^2) \qquad (36)$$

This formulation leads to a calculated threshold photoionization cross section of the H atom of 8×10^{-18} cm^2 ($Z = 1$, $IP = 13.6$, $\rho = 1$), whereas for comparison a more detailed calculation[31] gives 6.3×10^{-18} cm^2. In particular, we should note that for low ionization potentials the cross section increases just as the size of the orbital, which is proportional to $IP^{-\frac{1}{2}}$, and falls rapidly as the energy is increased above threshold as $(E/IP)^{-3}$.

Figure 6 shows a comparison of various experimental measurements and other theoretical calculations with the present theory. In each case, the cross section has been multiplied by $(IP/13.6\ eV)^{\frac{1}{2}}$ and divided by the number of electrons in the shell to be ionized, so that species with different ionization potentials can all be compared together. Considering the simplicity of the present calculation, the agreement is rather good.

Finally, Figure 7 shows our estimates of the photoionization cross section of the various rare gas excimers, each evaluated at its own emission maximum. The values are (within a factor of 2) as follows: Xe_2^*, 2×10^{-18} cm^2; Kr_2^*, 1.3×10^{-18}; Ar_2^*, 9×10^{-19}; Ne_2^*, 2.3×10^{-19}; and He_2^*, 2.1×10^{-19} cm^2. To arrive at these figures we have assumed an ionization potential of 4 eV for the various excimers. These ionization potentials are estimated to be accurate to ± 10%. A change of this magnitude in the ionization potential will result in a 25%

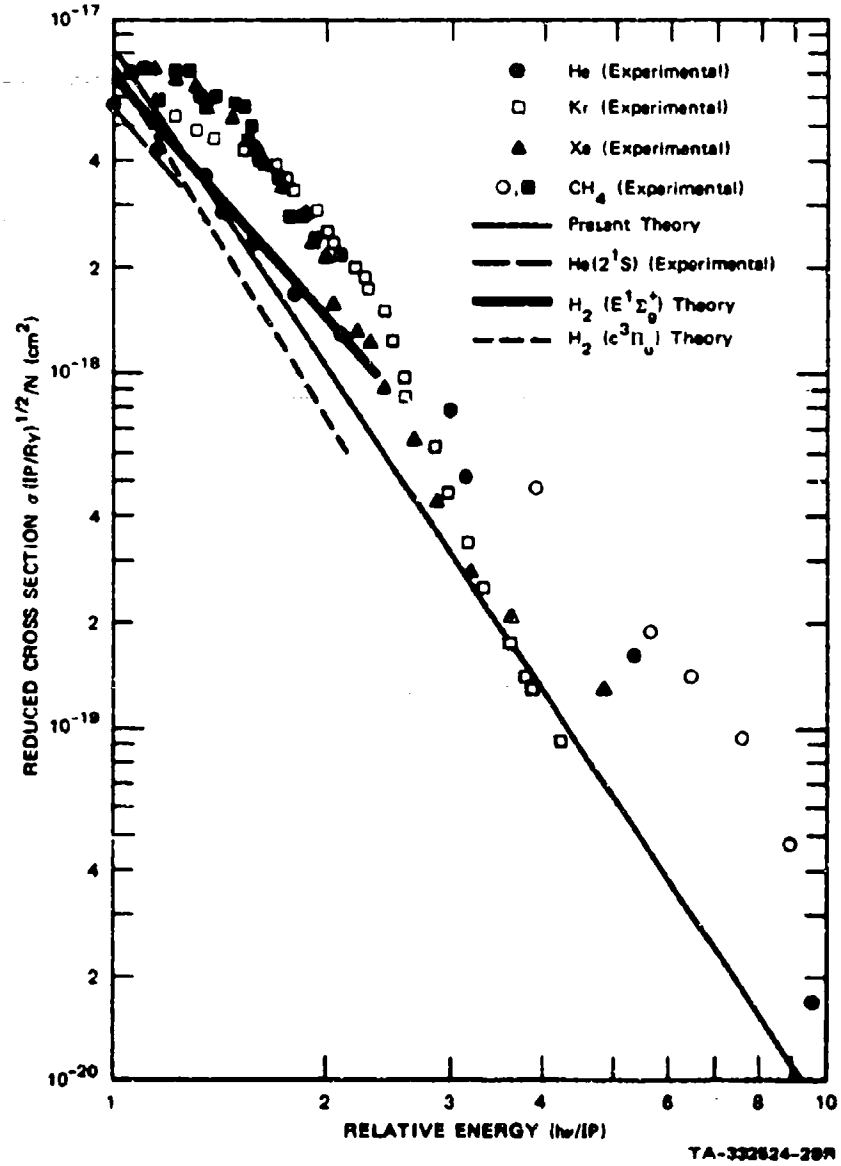

FIGURE 6 COMPARISON OF VARIOUS REDUCED PHOTOIONIZATION CROSS SECTIONS WITH PRESENT THEORY

He from reference 32, Kr and Xe reference 31, CH_4 from reference 33 and 34, He (2^1S) from reference 35, H_2 ($E^1\Sigma g$) and H_2 ($c^3\Pi_u$) from reference 30.

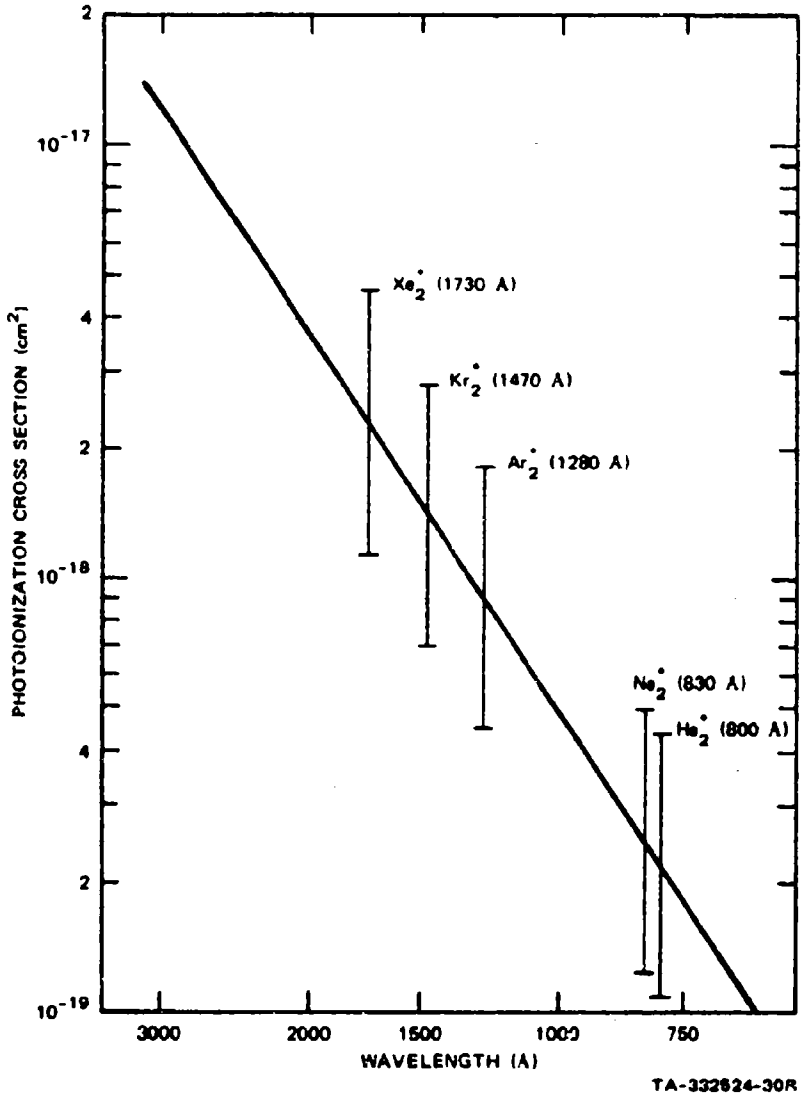

FIGURE 7 PREDICTED PHOTOIONIZATION CROSS SECTIONS FOR THE RARE GAS EXCIMERS

change in the cross section.

Absorption by Ground-State Molecules

Absorption of the 1750 Å continuum of xenon by transient ground-state xenon molecules has been measured by Koehler et al[6] (measurements of absorption near the 1470 Å atomic resonance line have also been reported[36]). The results are anomalous in the sense that the transient molecular population is proportional to the square of the number density N, and therefore the absorption coefficient should also obey that dependence. In the pressure range from 0 to 30 atm, however, these measurements show a linear dependence on N, namely,

$$I/I_o = \exp(-\alpha L) \qquad (37)$$

where $\alpha \cong 2.7 \times 10^{-23} N$. This linear dependence on density leads one to suspect an impurity. For example, either about 40 ppm of oxygen impurity or 5 ppm of water vapor could account for the observed absorption below 30 atm.

The molecular xenon absorption is expected to be somewhat smaller in magnitude for pressures less than 30 atm than the values measured. We can show this approximately by following the analysis of Hedges et al[37] and Phelps,[38] who show that the number of transient molecules capable of absorbing at the wavelength ν (corresponding to an internuclear distance R) is

$$N_M(\nu) = N^2 4\pi R^2 [d\nu/dR)] \exp [-V_1(R)/kT] \qquad (38)$$

where $V_1(R)$ is the repulsive ground-state potential, and $d\nu/dR$ is the variation of absorption frequency with internuclear distance ($\sim 4.5 \times 10^{22}$ Hz/cm for xenon). Taking $V_1 \cong 0.25$ eV at the internuclear distance of the well in the excimer potential ($R \cong 3.3$ Å), we find for $T = 300^\circ$ K that

$$N_M(\nu) \cong 2 \times 10^{-41} N^2 \Delta\nu. \qquad (39)$$

Now the absorption coefficient is

$$\alpha(\nu) \cong \frac{\lambda^2}{8\pi} A_{ul} \frac{\Delta N_{M(\nu)}}{\Delta\nu}$$

$$\cong 5 \times 10^{-45} N^2 \text{ cm}^{-1} \qquad (40)$$

Thus, at p = 30 atm ($N = 9 \times 10^{20}$), $\alpha_M < 0.005$ cm^{-1}. This compares with the measured value of $\alpha = 0.025$ cm^{-1}.

Any of the absorption mechanisms postulated above (i.e., by Xe_2, O_2, or H_2O) can account for the observed shift of wavelength of the xenon emission to longer wavelengths[4,6] with increasing pressure, since the absorption in each case becomes greater with decreasing wavelength.

At pressures above 30 atm, the xenon absorption increases very rapidly. This is probably due to scattering by multi-atom xenon "droplets" that grow in size and number as the density approaches its critical value.

V CONCLUSIONS

A model of the excitation of excimers in high pressure rare gases has been formulated on the basis of the electronic structure proposed for Xe_2 by Mulliken. This model includes the energy deposition, electron recombination, excimer formation, and relaxation processes, and finally, the radiative properties. Considerable progress has been realized in understanding the observed spontaneous emission characteristics of the vuv excimer bands over a wide range of pressures and excitation densities. The basic understanding realized in those studies is directly applicable to the on-going efforts to understand the properties of these transitions under lasing conditions.

On the basis of our studies we have reached the following conclusions.

(1) The $^1\Sigma_u^+$ excimer is the upper level of the lasing transition.

(2) The photoionization cross section of the $^3\Sigma_u^+$ excimer level probably exceeds its stimulated emission cross section. This would make the $^3\Sigma_u^+$ population act as an absorber of the singlet radiation.

(3) Rapid (electron induced) mixing of the $^1\Sigma_u^+$ and $^3\Sigma_u^+$ states is implied by the observed decay behavior. This would be a necessary condition to insure a population in the $^1\Sigma_u^+$ level sufficient for lasing.

(4) Excimer-excimer Penning ionization remains a significant limitation on laser efficiency.

(5) Quenching of the excimers by ground state atoms does not appear to be an important loss mechanism.

Considerable research remains to be done to fully understand and to fully realize the potential of these systems as vuv lasers and light sources. It is particularly important to establish the electronic state structure of the excited rare gas dimers, to determine rate constants or cross sections for many important collision processes, and to measure the radiative transition probabilities.

Considerable rate information is needed for the various collisional relaxation processes, excimer formation processes, and excimer-excimer ionization collisions. Of particular importance for the high density excitation cases are the low energy electron interactions with the excimers and other excited states. Electron temperature and density measurements of the plasmas would be valuable.

Radiative lifetimes of the $^3\Sigma$ and $^1\Sigma$ states need to be measured. The singlet state lifetime is most urgently needed, but it must be measured at low electron density and low pressure to avoid collisional mixing with the triplet level. Photoionization cross sections of the excimer states should be measured.

We can expect that as more and better information is developed

about these systems, it will be possible to design efficient and practical vuv sources, lasers, and energy transfer media based on the excimer states. Mainly because of the high efficiencies that can be attained, it can be expected that many practical applications will be realized in the areas of new laser developments and photochemistry.

REFERENCES

1. H. A. Koehler, L. J. Ferderber, D. L. Redhead, and P. J. Ebert, Appl. Phys. Lett. 21, 198 (1972).

2. J. B. Gerardo and A. W. Johnson, J. Quant. Elect. QE-9, 748 (1973).

3. P. W. Hoff, J. C. Swingle, and C. K. Rhodes, Optics Comm. 8, 128 (1973).

4. P. W. Hoff, J. C. Swingle, and C. K. Rhodes, Appl. Phys. Lett. 23, 245 (1973).

5. D. J. Eckstrom, R. A. Gutcheck, R. M. Hill, D. Huestis, and D. C. Lorents, "Studies of E-Beam Pumped Molecular Lasers," SRI MP-73-1, Semiannual Technical Report No. 2, Contract N00014-72-C-0478, Stanford Research Institute, Menlo Park, California (July 1973).

6. H. A. Koehler, L. J. Ferderber, D. L. Redhead, and P. J. Ebert, "Vacuum ultraviolet emission from high-pressure Xenon and Argon excited by high-current relativistic electron beams," to be published.

7. R. S. Mulliken, J. Chem. Phys. 52, 5170 (1970).

8. D. C. Lorents and R. E. Olson, "Excimer Formation and Decay Processes in Rare Gases," Semiannual Report No. 1, Contract N00014-72-C-0457, Stanford Research Institute, December 1972.

9. D. C. Lorents, R. E. Olson, and G. M. Conklin, Chem. Phys. Lett. 20, 589 (1973).

10. T. L. Gilbert and A. C. Wahl, J. Chem. Phys. 55, 5247 (1971).

11. E. U. Condon and G. H. Shortley, The Theory of Atomic Spectra, (Cambridge, 1935).

12. C. E. Moore, Atomic Energy Levels, Vol. 1,2,3, NBS Circular 467 (1949, 1952, 1958).

13. Y. Tanaka and K. Yoshino, J. Chem. Phys. 53, 2012 (1970).

14. E. V. George, private communication.

15. E. V. George and C. K. Rhodes, Appl. Phys. Lett. 23, 139 (1973).

16. G. W. Gear, Comm. A.C.M. 14, 176 (1971).

17. C. W. Gear, Comm. A.C.M. 14, 185 (1971).

18. C. E. Treanor, Math. Comp. 20, 39 (1966).

19. R. Boucique and P. Mortier, J. Phys. D. 3, 1905 (1970).

20. N. Thonnard and G. S. Hurst, Phys. Rev. A 5, 1110 (1972).

21. P. K. Leichner, Phys. Rev. A 8, 815 (1973).

22. P. K. Leichner and R. J. Ericson, "Time Dependence of the Vacuum Ultraviolet Emission in Krypton," to be published.

23. D. J. Bradley, M.H.R. Hutchinson, and H. Koetser, Optics Comm. 7, 187 (1973).

24. S. C. Wallace, R. T. Hodgson, and R. W. Dreyfus, Appl. Phys. Lett. 23,22 (1973).

25. J. B. Gerardo and A. W. Johnson, J. Chem. Phys. 59, 1738 (1973).

26. A. B. Callear and P. M. Wood, Tran. Faraday Soc. 67, 272 (1971).

27. A. W. Johnson and J. B. Gerardo, 25th Gaseous Electronics Conference, London, Ontario, October 1972, p. 154.

28. A. Burgess and M. J. Seaton, Monthly Notices Roy. Astron. Soc., 120, 121 (1960).

29. H. A. Bethe and E. Salpeter, Quantum Mechanics of One and Two Electron Atoms (Academic Press, New York, 1957), p. 308.

30. A. Cohn, J. Chem. Phys. 57, 2456 (1972).

31. J.A.R. Samson, Advances in Atomic and Molecular Physics, 2, 177 (1966).

32. J. F. Lowry, D. H. Tomboulian, and D. L. Ederer, Phys. Rev., 137, A1054 (1965).

33. N. Wainfan, W. C. Walker, and G. L. Weissler, Phys. Rev. 99, 542 (1955).

34. U. Fano and J. W. Cooper, Rev. Mod. Phys., 40, 441 (1968).

35. R. F. Stebbings, F. B. Dunning, F. K. Tittel, and R. D. Rundel, Phys. Rev. Lett., 30, 815 (1973).

36. I. V. Kasinshaya and L. P. Palozova, Opt. Spect. (USSR) 30, 458 (1971).

37. R.E.M. Hedges, D. L. Drummond, and A. Gallagher, Phys. Rev. A 6, 1519 (1972).

38. A. V. Phelps, "Tunable Gas Lasers Utilizing Ground State Dissociation," JILA Report No. 110, Univ. of Colorado, September 15, 1972.